Chem. Senses 36: 251–260, 2011
doi:10.1093/chemse/bjq120
Advance Access publication December 21, 2010

Different Profiles of Main and Accessory Olfactory Bulb Mitral/Tufted Cell Projections Revealed in Mice Using an Anterograde Tracer and a Whole-Mount, Flattened Cortex Preparation

Ningdong Kang[1], Michael J. Baum[1] and James A. Cherry[2]

[1]Department of Biology, Boston University and [2]Department of Psychology, Boston University, Boston, MA 02215, USA

Correspondence to be sent to: James A. Cherry, Department of Psychology, 64 Cummington Street, Boston University, Boston, MA 02215, USA. e-mail: jcherry@bu.edu

Accepted October 11, 2010

Abstract

A whole-mount, flattened cortex preparation was developed to compare profiles of axonal projections from main olfactory bulb (MOB) and accessory olfactory bulb (AOB) mitral and tufted (M/T) cells. After injections of the anterograde tracer, Phaseolus vulgaris leucoagglutinin, mapping of labeled axons using a Neurolucida system showed that M/T cells in the AOB sent axons primarily to the medial and posterior lateral cortical amygdala, with minimal branching into the piriform cortex. By contrast, M/T cells in the MOB displayed a network of collaterals that branched off the primary axon at several levels of the lateral olfactory tract (LOT). Collaterals emerging from the LOT into the anterior piriform cortex were often observed crossing into the posterior piriform cortex. M/T cells in the dorsal MOB extended fewer collaterals from the primary axon in the rostral LOT than did M/T cells from the anterior or ventral MOB. MOB M/T cells that projected to the medial amygdala did not do so exclusively, also sending collaterals to the anterior cortical amygdala as well as to olfactory cortical regions. This arrangement may be related to the ability of social experience to modify the response of mice to volatile pheromones detected by the main olfactory system.

Key words: axon collaterals, lateral olfactory tract, medial amygdala, PHA-L, piriform cortex

Introduction

Volatile environmental odorants are sensed by olfactory receptor neurons in the main olfactory epithelium that send axons via the olfactory nerve to glomeruli in the main olfactory bulb (MOB). Conversely, nonvolatile chemical cues are detected by receptor neurons in the vomeronasal organ (VNO) that project via the vomeronasal nerve to the accessory olfactory bulb (AOB). Secondary olfactory targets of the MOB and AOB have traditionally been described as nonoverlapping: whereas AOB mitral and tufted (M/T) cells send projections to the ''vomeronasal'' amygdala (medial amygdala, MeA; posterior medial cortical amygdala), MOB outputs extend more widely to sites within the olfactory cortex and to the ''olfactory'' amygdala, including the anterior cortical amygdala (ACo) and posterior lateral cortical amygdala (PLCo) (Broadwell 1975; Scalia and Winans 1975; Davis et al. 1978; Shipley and Adamek 1984; Martinez-Garcia et al. 1991; Carmichael et al. 1994; Jansen et al. 1998; Pro-Sistiaga et al. 2007). Recently, however, it was shown in mice that a subpopulation of M/T cells from the MOB project directly to the MeA, and these cells are preferentially activated by volatiles from urine of the opposite sex (Kang et al. 2009). These results suggest that information about social odorants detected by the main and accessory olfactory systems is sent monosynaptically to the MeA before being conveyed to areas in the hypothalamus that regulate species-typical behaviors.

Perhaps due to the difficulty in tracing axons over long distances, there have been few studies examining the routes taken by individual projection neurons from the MOB or AOB to targets in the olfactory cortex and amygdala. Over 25 years ago, Ojima et al. (1984) reconstructed the axonal trajectories of individual M/T cells injected intracellularly with horseradish peroxidase in the rabbit MOB to target sites within the anterior piriform cortex (APC). That and another study (Devor 1976) revealed that mitral cell primary axons branch extensively, sending collaterals to sites within the anterior olfactory nucleus, APC, and, in some cases, to the olfactory tubercle (Tu). These studies suggest that odors

that activate even a small fraction of M/T cells may nevertheless produce concurrent activation within multiple, distinct sites within the olfactory cortex. Left unresolved in these studies, however, was whether individual M/T cells send collaterals to both the APC and the posterior piriform cortex (PPC), areas that are believed to be functionally distinct (Kadohisa and Wilson 2006; Howard et al. 2009).

It has been suggested that instinctive responses to odors regulating reproductive and defensive behaviors in mice are mediated by parallel anatomical pathways that remain segregated until convergence in the hypothalamus (Choi et al. 2005). Although the extent to which the main and accessory olfactory systems supply the sensory input to these pathways has yet to be determined, one might predict, based on the observed segregation, that axonal fibers from MOB and/or AOB M/T cells that transmit information via the amygdala to the hypothalamus may be less likely to exhibit the degree of branching seen generally in M/T cells (Ojima et al. 1984). To examine this possibility, we examined axonal morphology in AOB and MOB M/T cells using a novel method that allowed visualization of axonal trajectories in a modified whole mount of the olfactory cortex and surrounding areas. Projections from both the MOB and the AOB run superficially in the LOT before exiting into their appropriate targets (Shipley and Adamek 1984; Inaki et al. 2004). We took advantage of this morphology to create a flattened cortex preparation that allowed us to map the axonal projections of M/T cells without having to reconstruct arbors of individual cells from adjacent histological sections. This method enabled us to address the following questions: 1) Is the extensive branching seen in MOB M/T cells also observed for AOB mitral cells? 2) Do MeA-projecting M/T cells from the MOB send collaterals to other targets? 3) Do the APC and PPC receive collaterals from the same MOB M/T cell? and 4) Do M/T cells located in the dorsal versus ventral MOB exhibit a similar degree of branching?

Materials and methods

Animals

Adult (8–12 weeks old) male Swiss Webster mice were purchased from Taconic Farms (Taconic) and housed in groups of 4. Animals lived under a 12:12 h light:dark cycle, and food and water were available at all times. All procedures were approved by the Boston University Charles River Campus Institutional Animal Care and Use Committee.

Procedures

Injection of anterograde neural tracers

Mice were anesthetized using 1% isoflurane vapor. The head was fixed in a stereotaxic instrument (David Kopf Instruments), and the skull was exposed, whereupon the skull landmarks (lambda and bregma) were set in the same horizontal plane. A small hole was drilled above the olfactory bulb, and using the intersection of the inferior cerebral vein, the hemispheric midline, and the dural surface as the reference point, Phaseolus vulgaris leucoagglutinin (PHA-L) (2.5% in 0.01 M phosphate buffer [PB], pH 8.0; Vector Laboratories), Fluoro-Ruby (dextran, tetramethylrhodamine, 10 000 MW, 5% in 0.01 M PB, pH 8.0; Molecular Probes), or Fluoro-Emerald (dextran, fluorescein, 10 000 MW 5% in 0.01 M PB, pH 8.0; Molecular Probes) were injected iontophoretically into the MOB in different experiments. Injection coordinates, expressed as the distances anterior to, lateral to, and below the reference point, were as follows—ventral MOB: 1.0, 0.8, and 2.2; dorsal MOB: 1.0, 0.8, and 0.2; anterior MOB: 1.2, 0.8, and 0.2; posterior lateral MOB: 0.81, 1.45, and 1.46; posterior medial MOB: 0.4, 0.27, and 2.8; and AOB: –0.29, 0.8, and 1.53. All injections were made using pulled glass micropipettes (tip diameter = 10–15 μm) and a constant current source (Stoelting). Injection pipettes were inserted at different orientations when targeting different parts of the MOB as well as the AOB in order to avoid damaging blood vessels. A +5 μA alternating current (7 s on and 7 s off) was applied for 15 min to deliver the tracer once the pipette was in place. Five minutes after the termination of each injection, the pipette was withdrawn while passing a –2 μA current. A piece of sterile aluminum foil was glued to the skull using cyanoacryester adhesive to seal the hole, and the skin was sutured over the skull. Seven days later, animals were sacrificed, whereupon brains were removed from the skull prior to being subjected to the flattening procedure and further processing (details below).

Whole-mount, flattened cortex preparation

Mice were deeply anesthetized with sodium pentobarbital (150 mg/kg) and perfused transcardially with 50 ml of ice-cold 0.1 M phosphate-buffered saline (PBS). The brain was removed without fixation, and the 2 hemispheres were separated. The olfactory bulbs were removed, soaked in 4% paraformaldehyde for 3 h, and then cryoprotected in 30% sucrose. Sagittal olfactory bulb sections were cut at 50 μm on a freezing microtome for later confirmation of PHA-L injection sites using immunohistochemistry; fluorescent tracer injection sites were localized from coronal MOB sections counterstained with TO-PRO-3 iodide (1:2000, Molecular Probes). The cerebellum, brain stem, diencephalon, and basal ganglia were dissected away from each unfixed hemisphere, and the remaining brain tissue was flattened onto a gloved fingertip using a paintbrush, taking care to unfold the temporal lobe, including the piriform cortex, entorhinal cortex, and amygdala. The flattened cortices were mounted onto coverslips with the pia against the glass and kept at room temperature (RT) for 20 min in order to facilitate attachment.

To create a map of the flattened brain with landmarks that could be referred back to an intact brain, 4 adult mice were fixed in a stereotaxic instrument, the skulls were exposed,

and lambda and bregma were adjusted to the same horizontal plane. Ink injections were made coronally at 1-mm intervals on the surface of the exposed cortex (Figure 1A–C). The ink-injected hemispheres were removed and flattened against a coverslip. The coverslip, with the brain tissue attached to the lower surface, was then elevated by 2 pieces of 1-mm-thick glass placed 3 cm apart on a slide. The coverslip, elevating pieces, and slide were glued together using cyanoacrylate ester adhesive (Figure 1D,E). With the lateral olfactory tract (LOT) and optic tract (OPT) serving as landmarks (Figure 1F), the APC, PPC, and Tu can be seen located dorsal, posterior, and ventral to the LOT, respectively, and the amygdaloid region can be seen located lateral to the OPT.

In animals that received MOB injections of the fluorescent anterograde tracers, Fluoro-Ruby and Fluoro-Emerald, cortices were flattened as described and immersed in 4% paraformaldehyde for 2 h at RT. Three holes (diameter of 0.5 mm) were carefully drilled through the cortex at 3 corners of the preparation to facilitate later alignment of adjacent sections. The flattened cortices were then cut at 150 μm on a vibratome in the horizontal plane (parallel to the surface of the brain), and the sections were soaked in Vectashield mounting medium (Vector Laboratories) overnight at 4 °C. Sections were mounted on microscope slides and coverslipped with the same medium.

To enable quantification of branching in a preparation where labeling of fibers was not subject to fading, immunocytochemistry was used following PHA-L injections to label axons and collaterals present in horizontal sections cut from flattened cortices. Free-floating sections were washed in 0.1% Triton-X100 in PBS (PBST). Following incubation with 40% methanol and 1% H_2O_2 in PBS for 10 min, sections were incubated for 2 h in PBST containing 5% rabbit serum (Vector Laboratories) at RT. Tissues were then incubated with goat anti-PHA-L antibody (1:4000, Vector Laboratories) in the blocking solution over 2 nights at 4 °C (total incubation 36 h). Sections were next washed in PBST and incubated with biotinylated rabbit anti-goat (1:400, Vector Laboratories) secondary antibody in rabbit solution for 3 h at RT. After PBST washes, sections were incubated in Avidin: Biotinylated enzyme Complex reagent (1:200, Vector Laboratories) for 3 h at RT. After washes with PBST and 0.05 M Tris–Cl buffer (pH = 7.6), tissues were placed in 3,3′-diaminobenzidine solution (DAB) (DAB kit, Vector Laboratories) for 5 min. Sections were then rinsed in ddH_2O, mounted on gelatin-coated slides, and dried in air overnight. Before coverslipping with Permount, sections were counterstained with 1% neutral red to help identify important anatomical landmarks used for mapping axonal arbor.

Microscopy and image processing

Flattened brains containing fluorescently labeled MOB and AOB M/T cell axons were inspected under an Olympus FluoView confocal microscope. Stacked optical slices were captured, collapsed in the *Z* dimension, and combined using

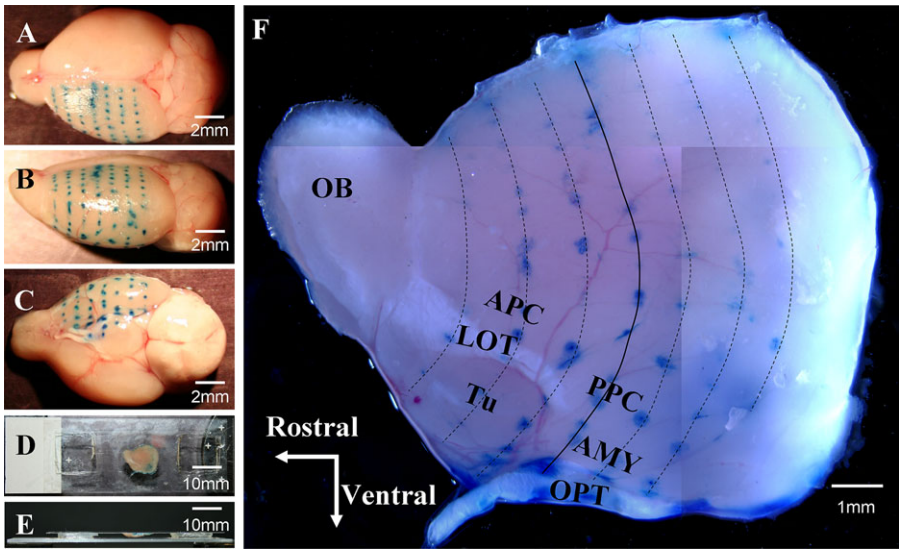

Figure 1 Preparation of a whole-mount, flattened cortex preparation: a mouse brain hemisphere was "unrolled" so that the curved brain surface was flattened. A mouse head was fixed in a stereotaxic instrument, the brain was exposed, and ink injections were made coronally at 1-mm intervals on the exposed left hemisphere to map landmarks that were later viewed in the flattened preparation. **(**Panels **A–C)** After removal of the brain from the skull, the dorsal, lateral, and ventral views of the left hemisphere are shown with rows of ink dots before the diencephalon was removed and the remaining cortex was flattened. **(**Panels **D** and **E)** Top and side views of a flattened mouse brain preparation resting on a slide beneath a coverslip. **(**Panel **F)** A flattened left hemisphere is shown at a higher magnification. The solid dark blue line delineates the coronal plane at bregma in the rostral–caudal dimension. The light blue lines delineate other coronal planes at 1-mm intervals rostral and caudal to bregma. The olfactory bulb (OB) is on the left and the lateral olfactory tract (LOT) extends from the OB caudally to the cortex. The anterior (APC) and the posterior (PPC) are dorsal to the LOT, whereas the olfactory tubercle (Tu) is ventral to the LOT. The amygdala (AMY) is positioned between the PPC and the OPT.

the Image J program (version 3.2, provided by National Institutes of Health). Light images of immunoreactive PHA-L–stained axons and collaterals were captured with an Olympus microscope equipped with a Nikon DXM1200 digital camera. Because olfactory bulbs were removed and sectioned for histological determination of injection sites, tracing of individual primary M/T cell axons and associated collaterals could not be followed to the cell body of origin. Rather, primary axons were traced at the point where the rhinal fissure and LOT begin to meet. Drawings, tracings, and montages were made using a Nikon E600 microscope (×60 objective, bright field) and a Neurolucida tracing system (Micro Brightfield). Functions (cropping, arranging, merging, and labeling) in Adobe Photoshop CS (version 8.0) were used to prepare all figures. Specific cortical and amygdaloid subnuclei were delineated based on their position relative to the middle cerebral artery, LOT, and Tu, as well as their appearance after neutral red counterstaining.

Results

Fluorescent tracers were used to reveal the overall pattern of axonal trajectories in the flattened cortex. Because a primary goal was to describe the morphology of MeA-projecting M/T cells, injections were aimed at the posterior lateral and posterior medial region of the MOB, sites where MeA-projecting M/T cells were previously localized (Kang et al. 2009). To increase the likelihood of successful injections, Fluoro-Ruby and Fluoro-Emerald were injected into different sites in each MOB of each subject. Successful injections were found in a total of 4 hemispheres (n = 3 mice). Using the flattened whole-mount preparation, axons labeled with either red or green tracer can be seen running along the extent of the LOT (Figure 2). Note that the appearance of yellow in Figure 2A, which typically depicts colocalization of the 2 tracers, is an artifact of stacking multiple individual Z-projection images taken every 40 µm. Figure 2B shows a single slice near the surface of the APC clearly revealing single-labeled red or green fibers with no colocalization of tracer but also displaying many nonneuronal cells dispersed in the pia that were labeled with both tracers (yellow). A similar labeling of such cells, perhaps caused by spread via the vasculature, is also seen in other published works using fluorescent tracers (Mohedano-Moriano et al. 2007; Pro-Sistiaga et al. 2007).

At the caudal end of the LOT, branches of axons cover the nucleus of the LOT (nLOT) and the MeA, confirming that posterior lateral and posterior medial MOB M/T cells project to the MeA via the LOT and that the axonal branches terminating in the MeA are the direct extensions of the labeled axon shafts. Fluorescently labeled axons reached the MeA in all 4 hemispheres studied with this method. In addition, numerous collaterals can be seen branching off axon shafts running in the LOT into various cortical regions. In the piriform cortex, primary axon collaterals tend to run

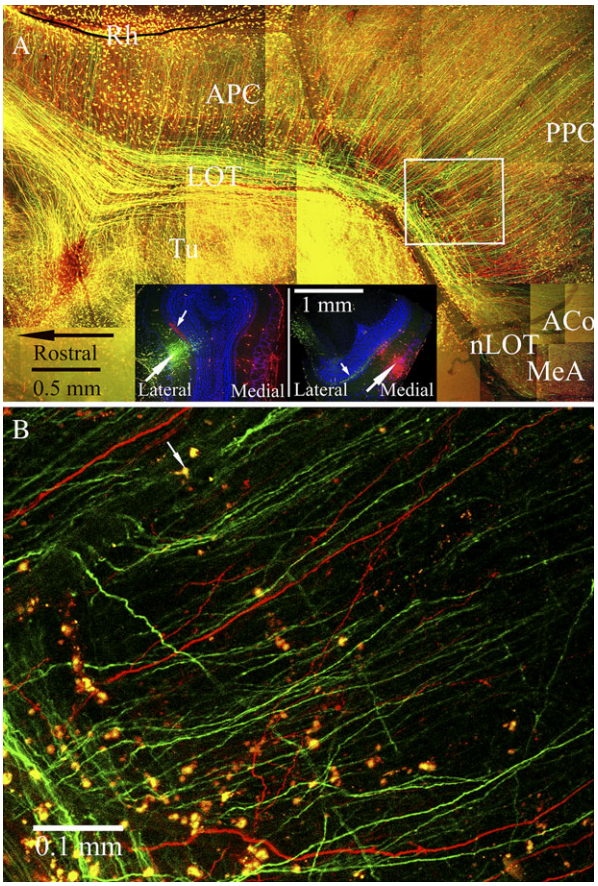

Figure 2 **(A)** M/T cell axons labeled by fluorescent anterograde tracers are shown in a montage of confocal images constructed from a 150-µm-thick horizontal section cut from a representative flattened cortex preparation. Panel insets show coronal sections from the same olfactory bulb of a male mouse in which iontophoretic injections of Fluoro-Emerald (green) and Fluoro-Ruby (red) were placed into the posterior lateral (left inset) and posterior medial (right inset) regions. Counterstain with TO-PRO-3 is depicted by blue pseudocolor. Tracer injection sites are indicated by large white arrows; small white arrows point to terminals in the internal plexiform layer that arise from intrabulbar mirror site projections (Schoenfeld et al. 1985). In the main panel, the LOT is filled with M/T cell axon shafts, which appear yellow due to the overlay of individual confocal images **(**see explanation for panel B below**)**. Numerous primary collaterals of M/T cell axons branch dorsally at right angles from the LOT toward the rhinal fissure (Rh). Some of these LOT collaterals can be seen entering the APC and extending deep into the PPC. Axonal branches targeting the ACo and the anterior MeA extend from the caudal end of the LOT. Axonal collaterals labeled by tracer injections into the medial and lateral MOB intermingle in all parts of the APC, the PPC, and the nucleus of the lateral olfactory tract (nLOT). (**B**) A single optical section from the boxed area in panel (A) is shown at high magnification to demonstrate that the yellow appearance of fibers in the LOT in panel (A) is not due to colocalization of both tracers within the same fibers. Individual fibers are either red or green; the impression in panel (A) that fibers colocalize the 2 tracers is due to overlap of red and green (represented by yellow) after stacking individual Z-projection slices, which varied in number depending on the thickness of the tissue. (e.g., in panel A, 4 optical sections were stacked in the region of the white box but up to 12 sections were stacked in some areas along the LOT.) A small arrow points to a yellow cell (labeled by both tracers). These cells were distributed in the pia and lack neuronal features (no dendrites or axons).

parallel to each other. In the APC, collaterals leave the LOT at a right angle toward the rhinal fissure, gradually assuming a diagonal orientation as they descend caudally. The areas of the piriform cortex that are above and posterior to the LOT are widely accepted as the APC and PPC, respectively (Price 1973; Johnson et al. 2000; Neville and Haberly 2004). Both the APC and the PPC can be seen in the flattened cortex preparation, and collaterals that first branch from the LOT into the APC are clearly seen entering and extending deep into the PPC (Figure 2A), indicating that the APC and PPC share the same MOB M/T cell collaterals. Toward the caudal end of the LOT, collaterals are seen that run to the ACo and extend to the PLCo. Some M/T cell collaterals exit the LOT and enter the medial portion of the Tu (Figure 2A); however, these collaterals angle sharply and adhere to a natural crease in the tissue upon entering the Tu and could not be followed easily.

Mapping of single axons and associated collaterals was carried out in sections cut from the flattened cortex of mice that received single injections of PHA-L into either the AOB or the dorsal or ventral MOB. The labeling seen in these preparations is shown for one example in which PHA-L was injected into the dorsal MOB (Figure 3, inserted image, upper left). A single labeled axon is shown in the LOT (Figure 3, panels 1–3), along with one primary collateral that branches into the PPC near the APC border (Figure 3, panels 4–12) and one secondary branch (Figure 3, panels 13–15) that emerges from the primary collateral and extends caudally across the PPC. In general, primary collaterals tended to branch out at right angles, leaving the LOT and extending toward the rhinal fissure in a relatively straight route. However, when inspected under high magnification, numerous small turns and enlargements of diameter give the primary collaterals a rougher appearance than the primary axon. Secondary branches leave the primary collaterals at various angles. These branches, whose diameters appear smaller than the primary collaterals, are often characterized by granule-like structures along their length. These morphological features were commonly seen in M/T cell projections from either the dorsal or the ventral MOB.

Detailed analysis of axonal branching in PHA-L–labeled material was accomplished in 2 ways, depending on the density of labeling. In a few cases where very few M/T cells were labeled, a complete characterization of a primary axon with associated collaterals was possible. For the AOB, the complete axonal arbor was delineated for 3 M/T cells (from 2 hemispheres of 2 animals). These cells displayed little branching until reaching the MeA, where numerous branches could be seen. For one of these cells, however, in addition to extensive branching in the MeA, multiple collaterals can also be seen in the ACo, a region that has been documented as receiving AOB input in rats (Pro-Sistiaga et al. 2007) but not in mice (Kang et al. 2009) (Figure 4A). Axonal arbors from 3 MOB M/T cells (from 3 hemispheres of 3 animals) were similarly characterized. In general, these MOB cells displayed an elaborate pattern of branching that targeted regions throughout the olfactory cortex. In one subject that received a PHA-L injection into the dorsal MOB, a single axon shaft is shown that branched extensively, with collaterals reaching sites in the APC, PPC, ACo, MeA, and PLCo (Figure 4B).

To describe more fully the pattern of branching in MOB M/T cells that project to the MeA, in some animals with a low density of PHA-L–labeled axons, collaterals found in the MeA were mapped retrogradely to the primary axon shaft located in the caudal segment of the LOT (n = 11 primary axons from 3 animals; Figure 4C). Collaterals from these primary axon shafts were observed that targeted the ACo (7 axons), PLCo (2 axons), and PPC (3 axons). These observations reveal that at least some of the MeA-projecting M/T cells in the MOB do not form a dedicated pathway to the MeA; rather, these cells send branches to numerous, additional sites in the olfactory cortex.

In other preparations with more labeled fibers, it became difficult to describe accurately the complete arborization patterns of individual cells. Nevertheless, in cases where there were fewer than approximately 10 labeled primary axons, it was possible to trace the projection pathways of identified axons for long distances. In these cases, the frequency with which axon shafts extended collaterals could be determined by tracing branching points along segments of the axon shafts running in the LOT. To assess whether branching differed among M/T cells originating in the dorsal versus ventral MOB, 27 segments of axon shafts were traced in 7 hemispheres (n = 7 subjects) following dorsal MOB PHA-L injections and 12 segments of axon shafts were traced in 3 hemispheres (n = 3 subjects) following ventral MOB PHA-L injections. The average length (mean ± standard error of the mean [SEM]) of these axon shaft segments was 703 ± 72 and 766 ± 128 μm for axons labeled by dorsal and ventral MOB injections of PHA-L, respectively. The frequency of axonal branching, calculated as the mean (±SEM) number of branching points occurring per 1000 μm, was 3.01 ± 0.22 and 4.14 ± 0.96 for dorsal and ventral M/T cells, respectively ($P > 0.05$ by t-test). Thus, by this analysis, dorsal and ventral M/T cells did not differ with respect to branching frequency.

The majority of the specimens created using PHA-L injections followed by DAB staining were intensely labeled, rendering it impossible to trace reliably single axon shafts for a long distance. In order to obtain quantitative data from this material, a collateral index was computed at 9 positions along the extent of the LOT following injections of PHA-L into 3 different regions of the MOB (Figure 5A–C) or into the AOB (Figure 5D). To establish these positions in each animal, landmarks representing the beginning and end of the LOT were identified using the point where the dorsal edge of the LOT and the rhinal fissure began to join and the point where the LOT transformed into the nLOT, respectively. Once these boundaries were located, the LOT was separated into 7 segments of identical length. The eighth

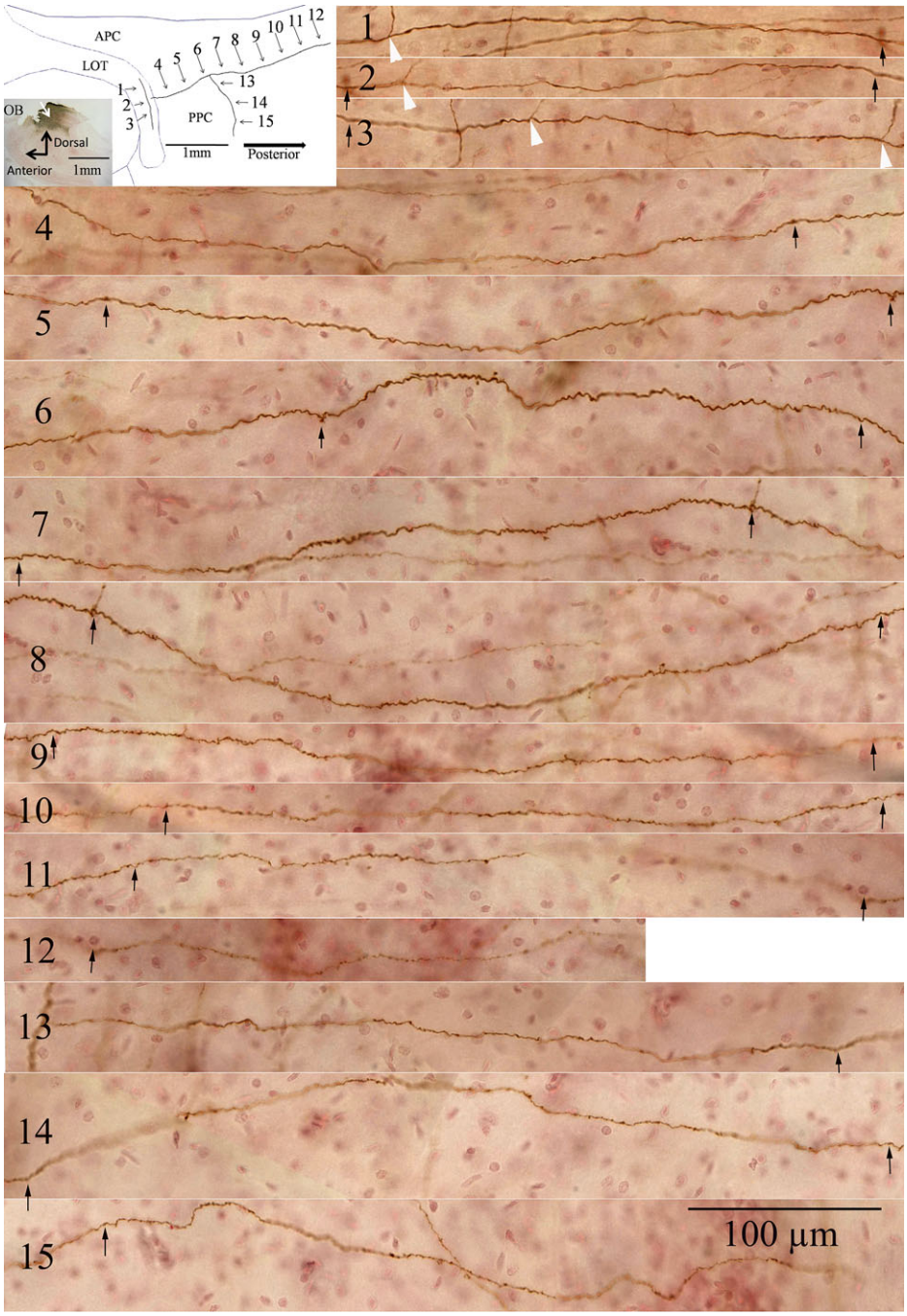

Figure 3 A single primary axon, along with one primary and one secondary collateral from the same axon, are shown from a flattened cortex preparation following immunocytochemical visualization of the anterograde tracer, PHA-L injected 7 days earlier into the dorsal MOB. Inset (upper left): the illustration shows segments from the primary axon shaft in the LOT (arrows 1–3), a primary collateral from this axon (arrows 4–12), and a secondary collateral that branches from the primary collateral (arrows 13–15). Landmarks shown are the LOT and APC and PPC. The tracer injection site from a sagittal section of the olfactory bulb (OB) is shown in the bottom left of the inset. The main figure (panels 1–15) displays the labeled axon (panels 1–3) and collaterals (primary, panels 4–12; secondary, panels 13–15) in a series of images that correspond to the segments shown in the inset. Overlapping areas on the labeled axons in successive panels are indicated by black arrows placed at the left and right ends of each image. Other collaterals emerging from the primary axon shaft are marked by white arrowheads in panels 1–3.

segment was defined by the boundaries of the ACo, and the ninth segment represented the MeA. In order to correct for individual variation in PHA-L labeling, the number of primary axonal shafts was first determined in the rostral part of the LOT for each injected hemisphere. The collateral index was then computed for each hemisphere by dividing this number into the number of collaterals counted along each of the 9 segments of the LOT. Injections of PHA-L into

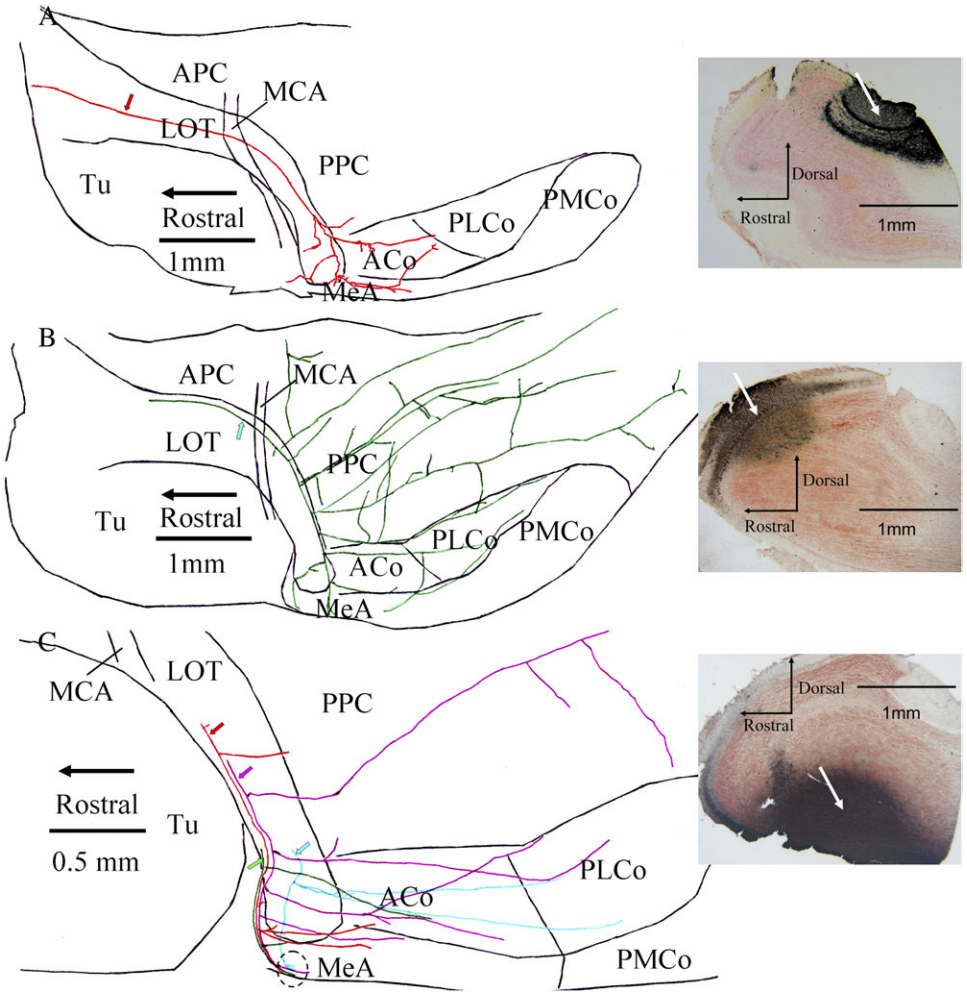

Figure 4 Neurolucida tracings from horizontal sections cut from flattened cortex show individual axonal processes from MOB and AOB M/T cells labeled by prior iontophoretic injections of the anterograde tracer, PHA-L; specific injection sites are shown in sagittal sections of the olfactory bulb on the right of each panel. **(**Panel **A)** A primary axon shaft (red arrow) was traced in the LOT after an injection of PHA-L into the AOB. Whereas no collaterals were seen to target either the APC or the PPC, branches from the primary shaft did extend into the ACo and anterior MeA. **(**Panel **B)** An axon shaft (green arrow) and an extensive arbor of collateral branches are shown after an injection of PHA-L into the dorsal MOB. Fibers widely infiltrate the PPC, as well as the ACo, PLCo, and MeA, yet avoid the posterior medial cortical amygdala (PMCo). **(**Panel **C)** 4 different axon shafts (red, purple, green, and blue arrows) were traced after an injection of PHA-L into the ventral MOB. Each of these primary shafts extended terminals to a small area within the MeA (dotted circle). Collateral branches also targeted the ACo and PLCo.

different subdivisions of the MOB or into the AOB differentially labeled axons and associated collaterals that exited the LOT into the piriform cortex and into subnuclei of the amygdala (Figure 5F). AOB M/T cells sent collaterals only to the ACo, the MeA, and the most caudal part of the PPC, whereas MOB M/T cells extended collaterals to widespread targets in the piriform cortex.

The degree of axonal branching exhibited by AOB and MOB M/T cells (using the collateral index values for each segment) was compared between injection groups (dorsal, ventral, or anterior MOB; AOB) using Kruskal–Wallis one-way analyses of variance (ANOVAs) computed separately for each LOT segment. Significant ($P < 0.05$) overall ANOVAs at each segment were followed by Mann–Whitney rank sum tests to compare injection group pairs. No collaterals from AOB M/T cells occurred in segments 1–6, so this injection group was included only in the ANOVAs run on segments 7–9. Several differences were found in the level of branching occurring in LOT segments depending on the injection site. In the most anterior parts of the APC (rostral to the middle cerebral artery; segments 1–3), the collateral index for dorsal MOB injections was significantly smaller than that for anterior and/or ventral MOB njections (H = 8.9, 7.8, and 8.6 for segments 1–3, respectively, all $P < 0.05$). In the most caudal segment, at the level of the MeA (segment 9), the collateral index for ventral MOB injections was significantly larger than that for dorsal MOB injections (H = 8.6, with 2 degrees of freedoms,

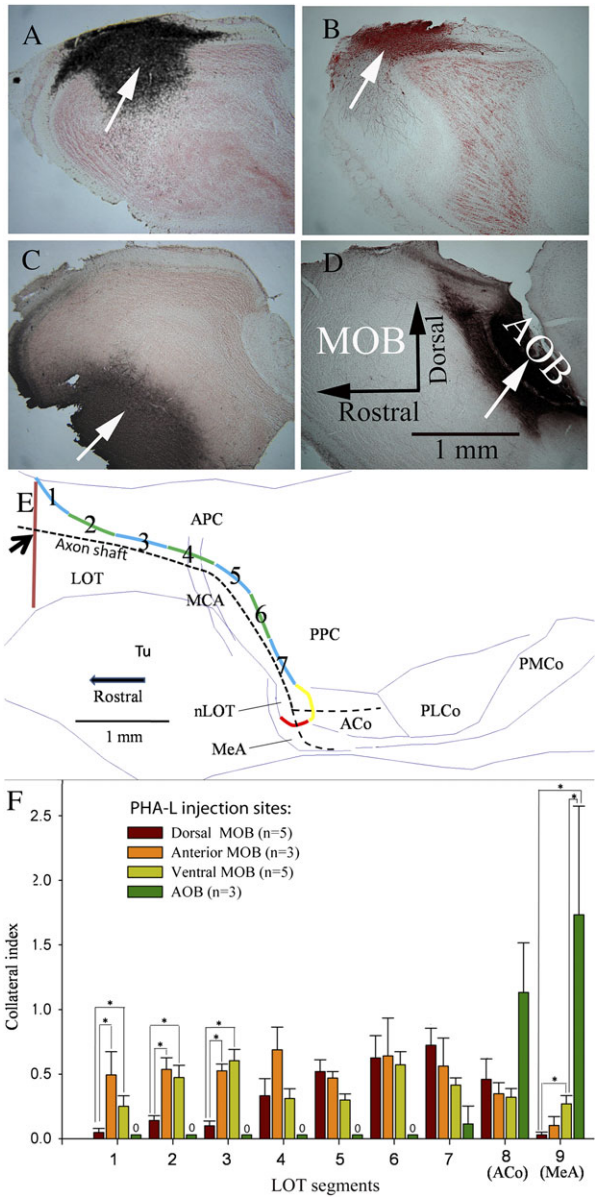

Figure 5 M/T cells in the AOB and MOB differ in the number of collaterals that branch from the primary axon shaft in the LOT into the APC and PPC, the ACo, and the MeA. Panels **(A–D)** PHA-L was iontophoretically injected into the dorsal (A), anterior (B), or ventral (C) MOB or into the AOB (D). **(**Panel **E)** A diagram shows where collaterals that emerged from primary axon shafts were counted (dashed black line). First, a vertical line (brown) drawn across the LOT shows where the APC first appears; the total number of labeled primary axon shafts that intersected this line (at the black arrow) were determined. The dorsal edge of the LOT was then subdivided equally into 7 segments (shown as alternating blue/green lines) as it passed through the piriform cortex; the caudal end at the level of the nLOT was further subdivided into 2 additional segments at the ACo (yellow) and MeA (red). All collaterals branching from axon shafts were counted and totaled for each of these numbered segments. For each subject, a collateral index for each segment was calculated as the number of collateral branches counted in each segment/the number of axon shafts counted at the proximal beginning of the LOT. (Panel F) Collateral index values (mean ± SEM) are graphed as a function of the location of branching along the LOT for 4 groups of mice previously given PHA-L injections into different sites in the MOB or AOB. The number of injected hemispheres (one per mouse) in each group is shown in parentheses. Asterisk (*) brackets indicate statistically significant comparisons ($P < 0.05$ by Mann–Whitney rank sum tests following a significant one-way Kruskal–Wallis nonparametric ANOVA for each segment).

$P < 0.05$). This result supports previous observations that PHA-L injections into the ventral portion of the MOB labeled a subpopulation of M/T cells that projected directly into the MeA (Kang et al. 2009). Also in segment 9, M/T cells in the AOB displayed significantly more branches than either dorsal or ventral MOB M/T cell groups ($H = 12.7$, $P < 0.05$). Collateral indices after PHA-L injections into the anterior and ventral MOB did not differ at any LOT segment.

Discussion

Projections from MOB and AOB M/T cells to forebrain targets have been previously studied using conventional anterograde and retrograde tracing techniques in many species, including mouse, hamster, rat, rabbit, opossum, lizard, sheep, and monkey (Broadwell 1975; Scalia and Winans 1975; Davis et al. 1978; Shipley and Adamek 1984; Martinez-Garcia et al. 1991; Carmichael et al. 1994; Jansen et al. 1998; Pro-Sistiaga et al. 2007). A few studies in small mammals have demonstrated that multiple collaterals emerge from the primary axons of MOB M/T cells to various targets in olfactory cortex (Devor 1976; Ojima et al. 1984); however, tracing of axons and associated collaterals over long distances can be tedious and inaccurate when reconstructing from histological sections, making it difficult to characterize the trajectories of MOB efferents. In the current study, axon shafts as well as primary and secondary collaterals were clearly identified, enabling the paths of these efferents to be traced. We found that the axons labeled by MOB injections of PHA-L traveled for considerable distances in the LOT, with multiple branches extending into different parts of the forebrain, including the APC, PPC, lateral entorhinal cortex (LEnt), ACo, and MeA. Notably, collaterals from primary axon shafts that originated in the APC were routinely observed crossing into the PPC, indicating that both structures may have access to information transmitted by individual M/T cells.

This broad axonal projection profile of MOB M/T cells might be predicted from the functional results of a recent study showing that single odorants activate neuronal ensembles that are widely distributed in the piriform cortex (Stettler and Axel 2009). It has been reported that axons from M/T cells located in different MOB regions run in the LOT in a topographic fashion (Inaki et al. 2004; Walz et al. 2006), whereas, in general, their projection profile into the piriform cortex is not topographic (Devor 1976; Shipley and Adamek 1984; Walz et al. 2006). It has also been reported that retrograde tracer injected into different parts

of the olfactory cortices produced labeled M/T cells throughout the MOB, although there were differences (in terms of cell density) in the distribution of these labeled cells (Scott et al. 1980). Our results from both grouped data and from single axon tracing following dorsal versus ventral MOB injections of PHA-L also show that MOB M/T cells exhibit different profiles of cortical innervation, supporting the conclusion of Scott et al. (1980) that there is a weak topographic relationship between the location of M/T cells in the MOB and the prevalence of projection sites in olfactory cortices. Whereas injections of anterograde tracer into the anterior and ventral MOB labeled M/T cells that sent collaterals all along the length of the LOT, collaterals from dorsal M/T cells were observed much less frequently in the anterior (i.e., segments 1–3 in Figure 4F) relative to the posterior LOT (segments 4–7). With respect to the overall frequency of branching, however, we observed no differences between primary axons originating from M/T cells located in the dorsal versus ventral MOB: primary axons from M/T cells in both regions sent an equivalent number of collaterals to sites within the olfactory cortex.

Characterization of the geometry of the MOB M/T cell projections to olfactory cortex may provide clues to how information is passed from the MOB to olfactory cortex. Action potentials from MOB M/T cells first travel along the axon shaft and then propagate along the axon collaterals at branching points from the LOT. The speed at which action potentials propagate along axon shafts in the LOT is higher than that along the branching collaterals from axon shafts (Rodriguez and Haberly 1989). We speculate that the first cortical structure abutting the LOT (i.e., the ventral APC) would be activated by inputs from MOB M/T cells more quickly than cortical structures that receive collaterals from more caudal segments of the LOT (e.g., PLCo and LEnt). This is in agreement with electrophysiological evidence showing that in the LEnt, there is a longer latency to show field potentials evoked by electrical stimulation of the LOT than more rostral regions of the piriform cortex and ACo (Kajiwara et al. 2007).

Until recently, it was thought that the olfactory and vomeronasal subdivisions of the amygdala receive distinct MOB and AOB inputs (Broadwell 1975; Scalia and Winans 1975; Davis et al. 1978; Carmichael et al. 1994; Jansen et al. 1998). In the present study, we confirmed recent reports that MOB and AOB mitral cell inputs converge in the MeA (Pro-Sistiaga et al. 2007; Kang et al. 2009). We also found that MOB M/T cells that project to the MeA, like other MOB M/T cells, extend collaterals to additional targets including the ACo, PLCo, and the PPC. In contrast, axons from AOB M/T cells extend few collaterals until nearing termination in the MeA, whereupon branching both within the MeA and into the adjacent ACo is seen.

This latter finding contrasts with our previous report (Kang et al. 2009) that retrograde tracer injected into the ACo failed to label the AOB, suggesting that the ACo does not receive direct inputs from the AOB. Support for the present finding are corroborating results from the rat and sheep, in which injection of retrograde tracer into the ACo labeled M/T cells in the AOB (Pro-Sistiaga et al. 2007; Meurisse et al. 2009). It could be that AOB collaterals in the ACo are not present at a high enough density, are too small in diameter, or distribute in different lamina from MOB collaterals, all of which could prevent sufficient levels of tracer from being retrogradely transported to cell bodies for visualization following small injections of cholera toxin B tracer as performed in our previous report (Kang et al. 2009). However, we also cannot exclude the possibility that labeling of axonal collaterals in the ACo following injections of anterograde tracer into the AOB was due to tracer that leaked along the injection tract. To avoid the inferior cerebral vein, deposition of tracer into the AOB required passage of a glass micropipette through the region of the MOB necklace glomeruli, which surround the AOB (Shinoda et al. 1989; Hu et al. 2007). Because it is unknown whether/how M/T cells associated with these necklace glomeruli project to the piriform cortex and ACo, the possibility exists that M/T cells associated with these glomeruli contributed to the labeling we observed in the ACo. More study will be required to resolve whether there are direct projections from AOB M/T cells that reach the ACo.

The observation that M/T cells in the AOB and MOB both target the MeA and the ACo raises the possibility of a more pronounced functional interaction between these 2 olfactory systems than has previously been realized. One context in which this might occur involves the attraction of female mice to male urinary volatiles. Nonvolatile male urinary odors, which are detected by the VNO and processed via the AOB, are intrinsically attractive to female mice (they show nasal investigation) in the absence of any prior experience with these odors. Without such experience, female mice typically fail to approach male urinary ''volatiles'' that are presumably detected by the main olfactory epithelium and processed via the MOB. Females are attracted to male urinary volatiles only after prior experience with nonvolatile urinary signals from males (Martinez-Garcia et al. 2009), perhaps because of the association of odor inputs from the main and the accessory olfactory systems in the MeA and/or ACo.

Funding

National Institutes of Health (R01 DC 008962).

Acknowledgements

Thanks to Dr Douglas Rosene of the Boston University Medical School, who generously made the Neurolucida tracing system available.

References

Broadwell RD. 1975. Olfactory relationships of the telencephalon and diencephalon in the rabbit. I. An autoradiographic study of the efferent connections of the main and accessory olfactory bulbs. J Comp Neurol. 163:329–345.

Carmichael ST, Clugnet MC, Price JL. 1994. Central olfactory connections in the macaque monkey. J Comp Neurol. 346:403–434.

Choi GB, Dong HW, Murphy AJ, Valenzuela DM, Yancopoulos GD, Swanson LW, Anderson DJ. 2005. Lhx6 delineates a pathway mediating innate reproductive behaviors from the amygdala to the hypothalamus. Neuron. 46:647–660.

Davis BJ, Macrides F, Youngs WM, Schneider SP, Rosene DL. 1978. Efferents and centrifugal afferents of the main and accessory olfactory bulbs in the hamster. Brain Res Bull. 3:59–72.

Devor M. 1976. Fiber trajectories of olfactory bulb efferents in the hamster. J Comp Neurol. 166:31–47.

Howard JD, Plailly J, Grueschow M, Haynes JD, Gottfried JA. 2009. Odor quality coding and categorization in human posterior piriform cortex. Nat Neurosci. 12:932–938.

Hu J, Zhong C, Ding C, Chi Q, Walz A, Mombaerts P, Matsunami H, Luo M. 2007. Detection of near-atmospheric concentrations of CO2 by an olfactory subsystem in the mouse. Science. 317:953–957.

Inaki K, Nishimura S, Nakashiba T, Itohara S, Yoshihara Y. 2004. Laminar organization of the developing lateral olfactory tract revealed by differential expression of cell recognition molecules. J Comp Neurol. 479: 243–256.

Jansen HT, Iwamoto GA, Jackson GL. 1998. Central connections of the ovine olfactory bulb formation identified using wheat germ agglutinin-conjugated horseradish peroxidase. Brain Res Bull. 45:27–39.

Johnson DM, Illig KR, Behan M, Haberly LB. 2000. New features of connectivity in piriform cortex visualized by intracellular injection of pyramidal cells suggest that "primary" olfactory cortex functions like "association" cortex in other sensory systems. J Neurosci. 20:6974–6982.

Kadohisa M, Wilson DA. 2006. Separate encoding of identity and similarity of complex familiar odors in piriform cortex. Proc Natl Acad Sci U S A. 103:15206–15211.

Kajiwara R, Tominaga T, Takashima I. 2007. Olfactory information converges in the amygdaloid cortex via the piriform and entorhinal cortices: observations in the guinea pig isolated whole-brain preparation. Eur J Neurosci. 25:3648–3658.

Kang N, Baum MJ, Cherry JA. 2009. A direct main olfactory bulb projection to the 'vomeronasal' amygdala in female mice selectively responds to volatile pheromones from males. Eur J Neurosci. 29:624–634.

Martinez-Garcia F, Martinez-Ricos J, Agustin-Pavon C, Martinez-Hernandez J, Novejarque A, Lanuza E. 2009. Refining the dual olfactory hypothesis: pheromone reward and odour experience. Behav Brain Res. 200: 277–286.

Martinez-Garcia F, Olucha FE, Teruel V, Lorente MJ, Schwerdtfeger WK. 1991. Afferent and efferent connections of the olfactory bulbs in the lizard Podarcis hispanica. J Comp Neurol. 305:337–347.

Meurisse M, Chaillou E, Lévy F. 2009. Afferent and efferent connections of the cortical and medial nuclei of the amygdala in sheep. J Chem Neuroanat. 37:87–97.

Mohedano-Moriano A, Pro-Sistiaga P, Ubeda-Banon I, Crespo C, Insausti R, Martinez-Marcos A. 2007. Segregated pathways to the vomeronasal amygdala: differential projections from the anterior and posterior divisions of the accessory olfactory bulb. Eur J Neurosci. 25:2065–2080.

Neville RK, Haberly BL. 2004. Olfactory cortex. In: Shepherd GM, editor. The synaptic organization of the brain V. New York: Oxford University Press. p. 415–454.

Ojima H, Mori K, Kishi K. 1984. The trajectory of mitral cell axons in the rabbit olfactory cortex revealed by intracellular HRP injection. J Comp Neurol. 230:77–87.

Price JL. 1973. An autoradiographic study of complementary laminar patterns of termination of afferent fibers to the olfactory cortex. J Comp Neurol. 150:87–108.

Pro-Sistiaga P, Mohedano-Moriano A, Ubeda-Banon I, Del Mar Arroyo-Jimenez M, Marcos P, Artacho-Perula E, Crespo C, Insausti R, Martinez-Marcos A. 2007. Convergence of olfactory and vomeronasal projections in the rat basal telencephalon. J Comp Neurol. 504:346–362.

Rodriguez R, Haberly LB. 1989. Analysis of synaptic events in the opossum piriform cortex with improved current source-density techniques. J Neurophysiol. 61:702–718.

Scalia F, Winans SS. 1975. The differential projections of the olfactory bulb and accessory olfactory bulb in mammals. J Comp Neurol. 161:31–55.

Schoenfeld TA, Marchand JE, Macrides F. 1985. Topographic organization of tufted cell axonal projections in the hamster main olfactory bulb: an intrabulbar associational system. J Comp Neurol. 235:503–518.

Scott JW, McBride RL, Schneider SP. 1980. The organization of projections from the olfactory bulb to the piriform cortex and olfactory tubercle in the rat. J Comp Neurol. 194:519–534.

Shinoda K, Shiotani Y, Osawa Y. 1989. "Necklace olfactory glomeruli" form unique components of the rat primary olfactory system. J Comp Neurol. 284:362–373.

Shipley MT, Adamek GD. 1984. The connections of the mouse olfactory bulb: a study using orthograde and retrograde transport of wheat germ agglutinin conjugated to horseradish peroxidase. Brain Res Bull. 12: 669–688.

Stettler DD, Axel R. 2009. Representations of odor in the piriform cortex. Neuron. 63:854–864.

Walz A, Omura M, Mombaerts P. 2006. Development and topography of the lateral olfactory tract in the mouse: imaging by genetically encoded and injected fluorescent markers. J Neurobiol. 66:835–846.